 doi:10.20944/preprints202003.0357.v1

# Neuropeptide Y expression confers Benzo[a]pyrene induced DNA damage and microtubule disruption in human neuroblastoma SH-SY5Y cells

Manorama Patri*

Neurobiology Laboratory, Department of Zoology, School of Life Sciences,

Ravenshaw University, Cuttack, Odisha, India

Running head: NPY expression protects benzo[a]pyrene-induced cell cycle arrest through microtubule disruption

*Corresponding Author

Dr. Manorama Patri

Neurobiology Laboratory

Department of Zoology

School of Life Sciences, Ravenshaw University, Cuttack-753003

Odisha, India

Email ID: mpatri@ravenshawuniversity.ac.in

 doi:10.20944/preprints202003.0357.v1

**Abstract**

Benzo[a]pyrene (B[a]P), is a family member of polycyclic aromatic hydrocarbons and a widespread environmental pollutant and neurotoxicant that contribute to the development of cancer. Microtubules are polymers of tubulin that form part of the cytoskeleton and target for anticancer drugs. Furthermore, NPY significantly increased the percentage of cells in S and G2/M phases. However, little is known about the specific role of NPY in proliferation and the underlying protective mechanism remains unclear. Hence, the aim of this work was to investigate the effect of B[a]P on SH-SY5Y neuroblastoma cells and to explore the potential mechanism for alteration of tubulin-microtubule equilibrium causing mitotic arrest and NPY expression. The present findings showed B[a]P treatment significantly increase number of SH-SY5Y cells in S and G2/M phase as compared to G1 phase and provokes cell cycle arrest that correlated with significant decrease in G0/G1 cells. Immunofluorescence study showed significantly distorted tubulin arrangement from metaphasic plate in formation of bipolar mitotic spindle apparatus. Further, higher doses of B[a]P treatment lead to chromosomal abnormalities accompanied by DNA damage due ROS causing oxidative stress showing significant decrease in tubulin protein around spindle. The results of present study demonstrated that NPY exerts a proliferative and protective effect on B[a]P-induced oxidative stress in a dose-dependent manner *in vitro* and importantly, these effects may be mediated via mitotic arrest and involved in spindle arrangement during cell division. Our findings addresses a novel pathological outcomes of B[a]P-induced NPY expression by oxidative stress through spindle abnormalities leading to microtubule disruption.

**Keywords:** Benzo[a]pyrene; Microtubule; Neuroblastoma; Cell cycle arrest, Neuropeptide Y

Preprints (www.preprints.org) | NOT PEER-REVIEWED | Posted: 24 March 2020 doi:10.20944/preprints202003.0357.v1

## 1. Introduction

Rising pollution load in the life sustaining ambient environment are primarily due to anthropogenic activities that might bring its adverse consequences on living organisms. The compounds like polycyclic aromatic hydrocarbons (PAHs) are reported to add a significant load of pollutants through incomplete combustion of fossil fuels [1,2]. Benzo[a]pyrene (B[a]P), a prototype of PAH is well known for its carcinogenic or mutagenic role [3,4], however in past decades, its neurotoxic potential is also well documented [5,6,7]. The neurotoxic potential of B[a]P is mainly achieved through neuromorphological alteration, cell cycle arrest, oxidative DNA damage, etc [8,9,10]. The environmental neurotoxicant like B[a]P undergoes metabolic breakdown into more potent toxicants by cytochrome P450 (CYP) enzymes and thus involves in formation of DNA adducts [11,12]. Metabolic activation of B[a]P and CYP induction are responsible to enhance oxidative stress conditions increasing physiological generation of reactive oxygen species (ROS) [13,14]. This anomalous condition in cell milieu induces changes in the cell cycle, DNA damage, chromosomal and mitotic aberrations. Several studies have highlighted B[a]P-induced ROS production as a consequence of the ability of its metabolites to enter redox cycles via direct and indirect mechanisms [15]. Because of the critical role of free radicals and ROS in the pathogenesis of cancer [16], the enhancement of oxidative stress resulting in the interaction between B[a]P metabolites and antioxidant enzyme activity [7]. The potential role of B[a]P inducing cell cycle arrest through cytoskeletal deformation like microtubule disruption is well reported [17,18]. Microtubules are arranged in a bipolar array with less dynamic minus-ends embedded at the pole and more dynamic plus-ends extending towards the spindle equator and cell cortex [19]. During early mitosis, the nuclear envelope breaks down; microtubules invade the nuclear space and attach to chromosomes at the kinetochore [20]. B[a]P induces microtubule disruption, but the cause behind this manifestation is limiting in literature. Microtubules are highly dynamic structures, which consist of α- and β-tubulin heterodimers and are involved in cell movement, intracellular trafficking, and mitosis with regulation of determination of cell morphology and differentiation.

The SH-SY5Y cells can be successfully differentiated to post-mitotic and more mature neuronal phenotypes. During several decades, the SH-SY5Y cell line has been used as an in vitro model system, detecting the impact of toxicants on mature and developing neurons [21]. Human neuroblastoma SH-SY5Y cells are immature

 doi:10.20944/preprints202003.0357.v1

neuroblasts characterized by their low differentiation, pyramidal shape, and obvious axons [21]. SH-SY5Y is a reliable model for studying the neurotoxic effect of B[a]P and for elucidating the mechanisms of NPY expression and as functional markers of neurons [22]. SH-SY5Y cells share some physiological functions with normal neurons [23]. Moreover, an increase in NPY production in the SH-SY5Y cell line can be associated with neurological diseases [24]. B[a]P alters the cytoskeleton, which is made up of three kinds of protein filaments: actin filaments, intermediate filaments and microtubules, and other associated proteins (tubulin) interfere with the tubulin-stabilizing process [25]. During mitosis B[a]P metabolites hinders the formation of the mitotic spindle and causes DNA damage and it may also modulate proteins involved in the intracellular transduction pathways. B[a]P also interferes with the assembly of cell microtubule and, in dividing cells, arrests the cells in the G2-M phase. An abnormal spindle structure can be a consequence of B[a]P-induced DNA damage or directly originated by spindle poisons leading to cell cycle arrest [25]. B[a]P-induced multi-polar spindle and mitotic arrest coupled to reduced cell proliferation and also increased apoptotic death through mitosis. Alterations in the mitotic spindle apparatus play a major role in the generation of genomic instability through promoting chromosome mis-segregation and aneuploidy.

NPY is the most abundant neuropeptide in the mammalian central nervous system and plays important roles in different pathological conditions such as obesity, anxiety, depression, cognition, epilepsy, chronic pain and other neurodegenerative disorders [26-28]. It is usually found that in the peripheral nervous system, NPY is co-exists with norepinephrine in the large dense-core vesicles at nerve endings of the sympathetic system. A significant body of literature argues that the arcuate nucleus NPY neurons are involved in energy homeostasis [29]. Whereas, limited information exists regarding the relationship between metabolic activation of B[a]P and NPY over expression causing oxidative stress leading to cell cycle arrest, microtubule distortions and spindle arrangement during cell division. Elevated neuronal activity results in the altered expression of NPY and tubulin protein molecules that may ultimately lead to alterations in the morphology and physiology of hippocampal neurons [30]. These changes may reflect adaptive responses to physiological activation of neurons. NPY has been shown to be present within the neurons of the hippocampus [31,32]. We previously demonstrated that endogenous increase in NPY over expression in hypothalamus and hippocampus was associated with increase body weight oxidative

Preprints (www.preprints.org) | NOT PEER-REVIEWED | Posted: 24 March 2020 doi:10.20944/preprints202003.0357.v1

stress following B[a]P administration (i.v.) due its orexigenic effects in rats [33,34].

Hence, the present study was conducted to know whether B[a]P induced DNA damage and cell cycle arrest causing microtubule disruption plays a role in NPY expression in neuroblastoma cells. SH-SY5Y cell lines were differentiated by 10 µM retinoic acid, maintained and treated with different doses of B[a]P (2 and 4µM) for 24 hour. It has been hypothesized that B[a]P-induced oxidative stress and DNA damage leading to cell cycle alterations could be due to different mechanisms that involve the dynamic nature of tubulin protein resulting NPY expression in SHSY5Y cells.

## 2. Results

### 2.1. Dose dependency of Benzo[a]pyrene on cell viability and proliferation of SH-SY5Y cells

After the Undifferentiated (UD) and differentiated (D) SH-SY5Y cells were exposed to different concentration of B[a]P (1, 2, 4 µM) respectively, samples with 2, 4 µM showed different vulnerability compared to the control (Fig. 1). Morphology of B[a]P treated SH-SY5Y cells under microscope revealed that cells in the control group grew well and were spindle-shaped or triangular, with a high transmittance. The differentiated SH-SY5Y cells following 10µm RA treatment for 24 hr showed more resistant to B[a]P treatment with extensive cell elongation with neurite outgrowth. B[a]P treated cells in both UD and D groups showed a decreased density, loose arrangement, became long, thin, and with intercellular space (Fig. 1A & B). Higher doses of B[a]P after 24 hr treatment showed more potent effect on cell proliferation in SH-SY5Y (relative MTT value) in comparison to control. B[a]P at 4µm doses, the cytotoxicity analysis revealed 58% cell viability having MTT assay for 24 hr treatment period (Fig. 1B).

### 2.2 Effect of B[a]P on DNA damage using the comet assay in SH-SY5Y cells

The DNA damaging effect of B[a]P on SH-SY5Y cells was evaluated by single cell gel electrophoresis; which compares the percentage of DNA in comet tail with tail moment, a measurement of DNA damage (Fig. 2A). In separate sets of experiment, the SH-SY5Y cells were treated with different concentration of B[a]P for 24hr. After PI staining, the nuclei of control cells appeared very bright, round and with intact nuclei. Cells treated showed 2µm with a short tail, whereas 4 µm B[a]P with moderate amount of DNA damage having more percentage of DNA in the comet tail in both the doses in comparison to the control group (Fig. 2B). Percentage of DNA migration showing

Preprints (www.preprints.org) | NOT PEER-REVIEWED | Posted: 24 March 2020 doi:10.20944/preprints202003.0357.v1

increased tail moment length dose dependently after B[a]P treatment in SH-SY5Y cells (Fig. 2C).

**2.3. Flow cytometry analysis after B[a]P treatment**

B[a]P treatment for 24 hrs significantly affect the percentage distribution of SH-SY5Y cells in different stages of cell cycle (Fig. 3A). To better understand the mechanism of action, we examined cell cycle progression by flow cytometry in two different concentration of B[a]P in our experiment. The flow cytometry analysis of SH-SY5Y cells showed that the proportion of cells in S-phase increases significantly in both 2 & 4µM treated group. There was a significant decrease in proportion of cells in G1 phase of cell cycle in B[a]P 2µM and an increase in proportion of cells in G2/M phase of cell cycle as compared to control (Fig. 3B). On the other hand, there was a significant decrease in the percentage distribution of cells in G2/M phase different of cell cycle in 4 µM B[a]P treated group as compared to B[a]P 2 µM and control group.

**2.4. Immunofluorescence study of α-tubulin protein after B[a]P treatment in SHSY5Y cells**

The organization of the mitotic spindle was examined by indirect immunofluorescence using an antibody to α-tubulin and DAPI that stains chromatin. Different types of abnormalities of the mitotic spindle were observed in both the doses of B[a]P treated and control groups. The immunofluorescence study of microtubule arrangement (tubulin) was shown to be significantly distorted from the metaphasic plate following B[a]P treatment. Higher dose B[a]P 4 µM) have significant impact on microtubule arrangement leading to displacement of chromosomes from metaphasic plate as compared to B[a]P 2 µM. Disruption of the mitotic spindles in the cells occurred at much lower B[a]P concentrations than those required to cause a significant alteration of the interphase microtubule network (Fig. 4A). SHSY5Y cells treated with B[a]P (2 & 4µM) showed abnormal mitotic bipolar to monopolar spindles as well as unipolar and multipolar spindles with misaligned chromosomes around the spindle. Spindles formed had either unipolar or multipolar organization. The relative tubulin intensity was increased significantly when the cells were treated with 4µM B[a]P and the spindle had a multipolar configuration indicating that the majority of the tubulin were in polymerized fraction in the B[a]P-treated cells in comparison to control. At concentrations of 4µM B[a]P, it induced bundling of interphase microtubules and formation of granular tubulin aggregates. Quantitative analysis of mitotic spindle alterations such as bipolar, monopolar and multipolar were shown in control and B[a]P

Preprints (www.preprints.org) | NOT PEER-REVIEWED | Posted: 24 March 2020 doi:10.20944/preprints202003.0357.v1

treated SHSY5Y cells (Fig. 4B).

**2.5. Immunofluorescence analysis of B[a]P induced NPY protein expression in SH-SY5Y cells**

Phase-contrast, immunofluorescence of protein tubulin (red), nuclear stain DAPI (blue), and merged images of SH-SY5Y on cells are shown (Fig. 5A). Immunofluorescence staining results revealed that NPY expression significantly increased in B[a]P treated SH-SY5Y cells when compared with the control group ($p< 0.05$). No significant changes in NPY expression were visible in the low-dose B[a]P (2μM) containing SH-SY5Y cells, however, a significant increase of NPY expression were found after higher (4μM) doses of B[a]P treatment in SH-SY5Y cells ($p<0.01$). The measured fluorescence intensity of NPY protein expression was significantly higher in the high-dose of B[a]P treatment in SH-SY5Y cells in comparison to control group, reaching its lowest value under merged (Fig. 5B).

3.3 **Materials and Methods**

**3.1. Chemicals**

The chemicals used in this experimentation were procured from Sigma-Aldrich Chemicals (St. Louis, MO, USA), unless otherwise mentioned. The quantification of NPY was carried by peptide enzyme immunoassay kit (Bachem, Peninsula Laboratories Inc., San Carlos, CA).

**3.2. Benzo[a]pyrene Treatment**

The B[a]P was solubilised in DMSO and the working solution of 10 mM concentration was prepared in cell culture media. In our study, we used both undifferentiated (UD) and differentiated (D) cultures of early passage cells. Both SHSY5Y cells were seeded into 96-well plates at a density of $2x10^4$ cells/ well and grown until 80% confluence for a maximum of 10 passages. B[a]P were treated at 2 and 4 μM concentration dissolved in DMSO (0.01%) for 24h. Neuronal differentiation was induced by adding to the culture media 10 μM retinoic acid (RA) dissolved in DMSO (0.01% v/v) as negative controls and all the plates were renewed after every 24 hr of treatment. The morphological assessment of cells were analyzed by phase contrast microscope. The experiments were carried out according to Ravenshaw University ethical guidelines for the care and use of cell lines and laboratory animals. The experiments were approved by the Institutional Animal Ethics Committee (Regd. No.1927/Go/Re/S/16/CPCSEA).

Preprints (www.preprints.org) | NOT PEER-REVIEWED | Posted: 24 March 2020 doi:10.20944/preprints202003.0357.v1

### 3.3. Cell cultures, differentiation and cell proliferation

SH-SY5Y human neuroblastoma cell line was obtained from National Centre for Cell Science (NCCS, Pune, India) and maintained at 37ºC with 5% $CO_2$ in growth medium containing DMEM supplemented with 10% FBS, 0.01% penicillin and streptomycin antibiotic mix. The cells were sub-cultured after attaining 70% confluence. Cell viability depends on an intact cell membrane. As a check for B[a]P-induced acute cytotoxicity, the integrity of the membrane (cytotoxicity) was determined after 24 hr exposure with native or differentiated SH-SY5Y cells. B[a]P concentration used (2µM & 4µM) was selected on the basis of our cytotoxicity test (MTT assay) to assess the cell viability (Patri et al., 2019). For dose-dependence, B[a]P was given at a concentration of 1, 2 and 4 µM for 24 hours. The DMSO (<0.1% of final volume) was used as a negative control in all experiments. The treatment was conducted under low light and was repeated three times.

### 3.4. Single cell gel electrophoresis (Comet assay)

The comet assay was carried out under alkaline conditions as reported earlier [35] to evaluate DNA strand breaks in individual SHSY5Y cells. Microscope slides were pre-coated with 0.75% normal melting agarose and stored at $4^0$C. The cells were grown for 24hrs in DMEM medium supplemented with 10% FBS, incubated at 5% $CO_2$, and 37°C. In separate sets, the cells were treated with B[a]P for 24hrs, washed with PBS and resuspended in 90µL of molten agarose (1%) at $37^0$C. This cell suspension was uniformly spread over agarose pre-coated slides (as described above) and placed on ice in the dark for 10 min. When the agarose gel solidified, the slides with cells were transferred to chilled lysis buffer (1% *N* -lauryl-sarcosine, 2.5 M NaCl, 10mM Tris-HCl, 100mM $Na_2EDTA$, 1% TritonX-100, 10% DMSO at pH >10) for 1hr at $4^0$C. The slides were placed in alkaline (pH >13) electrophoresis buffer for 20 min and then electrophoresis was carried out at 1.0 V/cm, 300mA for 40 min in dark at $4^0$C. After electrophoresis, the alkali in gels was neutralized in buffer solution (0.4M Tris-HCl, pH 7.4) and immersed in ice cold ethanol at room temperature for 5min and air dried. Then the slides were stained with 2.5µg/mL of PI for 20 min at $4^0$C. To analyze the degree of DNA damage in single cells, the images were captured with the help of microscope (Axiovision, Carl Zeiss Germany) and additional DNA damage parameter such as tail moment (product of tail length and percentage of DNA in tail) were quantified as a fraction of the DNA in the tail using the image analysis system of Comet Score™ v1.5 (TriTek Corp., USA).

Preprints (www.preprints.org) | NOT PEER-REVIEWED | Posted: 24 March 2020 doi:10.20944/preprints202003.0357.v1

### 3.5. Effect of Benzo[a]pyrene on phases of cell cycle by flow cytometry

The effect of B[a]P treatment on cell cycle was evaluated on the basis of cellular DNA content as reported earlier [35]. SH-SY5Y was grown in 60mm plates containing DMEM and 10% FBS at 37ºC in 5% $CO_2$ for 24hr. After the cells were confluent, they were washed twice with PBS and then treated with B[a]P for 24hrs. After treatment, cells were trypsinized, rinsed with PBS, and fixed in ice-cold 70% ethanol for one hour at 4ºC. Fixed cells were then centrifuged for 5min at 3000 rpm to obtain cell pellet, which was re-suspended in 1ml DNA staining buffer [50 µg propidium iodide (PI) with 100µg RNase A and Triton X-100]. After 30min of incubation at 370C, the cells were analyzed in a flow cytometer (BDFACS Calibur, BD Bioscience, USA). About 10,000 ungated events were collected for PI cell fluorescence to determine the relative cell cycle distribution as cellular DNA content frequency histograms in three major phases of cell cycle such as (G1), intermediate (S), and second (G2/M). The average percentages of cells in G1, S and G2/M phases of cell cycles were estimated from three sets of experiments, each under control and treated conditions and the data were analyzed using Win MDI (WinMDI Software).

### 3.6 Effect of Benzo[a]pyrene on spindle morphology by immunofluorescence

Immunofluorescence analysis was performed as previously described [35]. Briefly, SH-SY5Y cells were seeded at 104 cells/well on poly-l-lysine-coated coverlids. The cells were cultured in DMEM containing 10% fetal bovine serum, in the presence or absence of B[a]P, followed by washing twice with PBS and fixation with 4% paraformaldehyde for 10 min. Subsequently, the cells were permeabilized with 0.1% Triton X-100 in PBS, treated with PBS containing 10% fetal bovine serum and 0.1 M lysine to block unspecific antibody binding, and finally incubated with the primary antibodies (Anti-α- tubulin) overnight at 4°C. After being washed with PBST (PBS with 0.025% Tween-20) three times, the cells were incubated with phycoerythrin (PE)-conjugated secondary antibody (1:300 in 1% BSA in PBS, donkey anti-goat Santa Cruz Biotechnology Cat# sc-3743) for 1 hr at room temperature. Thereafter, the cells in cover slips were washed once with PBST, followed by PBS; the cells were next counterstained with DAPI. The cover slips were then mounted on slides using Mowiol mounting media containing the anti-fade agent DABCO and left overnight in an incubator (5% $CO_2$, 37ºC). Finally, the cover slip edges were sealed and microscopic images (Carl Zeiss, Jena, Germany) taken at least 100 cells were analyzed and fluorescence intensity estimated by using Image J software.

Preprints (www.preprints.org) | NOT PEER-REVIEWED | Posted: 24 March 2020 doi:10.20944/preprints202003.0357.v1

### 3.7. NPY expression in SHSY5Y cells after Benzo[a]pyrene treatment by immunofluorescence analysis

Cultured SHSY5Y cells after B[a]P treatment were subsequently fixed by applying ice-cold methanol and acetone (1:1) for 10 minutes at 20°C, blocked, and incubated with the monoclonal rabbit anti-NPY antibodies (1:500 diluted with 1% BSA in PBS; Millipore, Bedford, MA) at room temperature for 1 hr. After being washed with PBST three times, the cells were incubated with phycoerythrin (PE)-conjugated secondary antibody (1:300 in 1% BSA in PBS) for 1 hr at room temperature. The cells in cover slips were washed once with PBST, followed by PBS; then cells were next counterstained with DAPI. Finally, the cover slip edges were sealed and microscopic images (Carl Zeiss, Jena, Germany) were taken by fluorescence microscope equipped with a charge-coupled digital camera and fluorescence intensity was estimated by using Image J software.

### 3.8. Statistical analysis

Data have been expressed as mean ±SEM and were analyzed for statistical significance by applying one-way analysis of variance (ANOVA) and post hoc analysis was done by Newman-Keul's test (Sigma Stat software, Jandel Scientific USA). The number of replicates for each experiment was three and difference below the probability level $p < 0.05$ was considered statistically significant.

## 4. Discussion

In this study, we show the temporal expression of the neuronal peptide NPY in SH-SY5Y human neuroblastoma cell lines, advancing previous studies on NPY expression in wistar rats (6,27). This study was conducted on SH-SY5Y human neuroblastoma cell lines to ascertain the possible link between the B[a]P induced oxidative stress and cycle arrest causing NPY expression with microtubule disruption due to ROS production. NPY is known to play an important role in neuroprotection. The advantages of using a clonal cell culture, such as SH-SY5Y cells, are that cultures will be consistent, easy to maintain, possess a human phenotype. Hence, it was hypothesized that B[a]P affect tubulin filaments via different mechanisms (e.g. by inducing oxidative stress) with the sequestration of the damaged tubulin monomers and part of the filaments in the granules in SH-SY5Y cells [36]. The use of two different concentration of B[a]P (2 µM and 4 µM) in the present study are higher than the actual concentrations (0.03–0.09 ng/g wet tissue) reported for healthy humans [37, 38]. These concentrations were chosen because of their relevance to environmental levels of these

Preprints (www.preprints.org) | NOT PEER-REVIEWED | Posted: 24 March 2020 doi:10.20944/preprints202003.0357.v1

PAHs in hazardous waste sites, former industrial sites, and exposure concentrations for 'at risk' populations such as smokers and occupationally exposed individuals [39,40]. The phase contrast images of SHSY5Y cultures at control cells showed no particular neurite outgrowth and the cells have a round shape, whereas B[a]P-treated cells showed significant number of short neurites. The result also showed differentiated SH-SY5Y cells respond differently to toxicants like B[a]P in higher and lower doses with different cell morphology. The present findings addresses the augmented expression of NPY in rat brain following exposure to B[a]P and its correlation with the orexigenic effects depending on the antioxidant activity [15,8,37].

Previous reports suggested that B[a]P exposure leads to cell cycle arrest with significant increase in the number of cells in S-phase of cell cycle [41,42]. Importantly, from late S phase to mitotic onset, the two fully duplicated centrosomes exhibit enhanced recruitment of pericentriolar material components that are essential for microtubule nucleation, a process termed centrosome maturation [41]. When accumulation of pericentriolar material becomes inaccurate at the centrosome, results in a functionally compromised mitotic centrosome with multipolar or disorganized spindles that may further promote mitotic arrest and cell death [41]. The result showed higher B[a]P concentration adversely affect cell cycle by increasing the proportion of cells in S-phase indicating cell cycle arrest [33, 43,44]. The findings of the present flow cytometry analysis after B[a]P treatment in SH-SY5Y human neuroblastoma cell lines showed a significant increase in proportion of cells in S and G2/M phases as compared to G1 phase of cell cycle. Further, at higher concentration, B[a]P has shown to significantly increase the cell arrest in S phase of cell cycle as compared to lower concentration. In our study, SH-SY5Y cells when exposed to B[a]P induced oxidative stress as demonstrated by the significant increase of S phase cell accumulation and by the activation of the B[a]P metabolites to the antioxidant responses. In the present study, we found exposure to B[a]P in SH-SY5Y human neuroblastoma cell lines causes cell cycle arrest leading to increase proportion of cells at S phase and it finds support from previous reports [42,43,44]. Hence, it seems possible that oxidative stress may represent an important component in the mechanism of action of B[a]P-induced DNA damage in SH-SY5Y cell lines. Result showed that SH-SY5Y cells respond strongly to oxidative stress in a manner that affects the cytoskeletal structure of the mitotic spindle, intracellular calcium regulation and tubulin protein alterations that appears to be one of the few cytoskeletal protein expressed following exposure to B[a]P [17].

 doi:10.20944/preprints202003.0357.v1

The higher concentration of B[a]P showed distorted microtubule arrangement at metaphasic plate. Immunofluorescence analysis of tubulin was shown to be significantly distorted from metaphasic plate in B[a]P treated SH-SY5Y neuroblastoma cells as compared to control, which are particularly relevant at the higher B[a]P concentrations and imply an alteration of the organization of the spindle structure. Our immunofluorescence study following B[a]P exposure to SH-SY5Y human neuroblastoma cell line showed significant alteration in metaphasic microtubule arrangement. Distorted tubulin arrangements also affect the chromosome arrangement at metaphasic plate leading to bipolar and multi-polar spindle arrangement. Higher concentration of B[a]P treatment have significant impact on tubulin arrangement in SH-SY5Y neuroblastoma cells. Disrupted microtubule arrangement following B[a]P exposure has also been previously reported [17]. The cell cycle arrest in SH-SY5Y human neuroblastoma cell line following exposure to B[a]P may possibly due to impaired metaphasic microtubule arrangement.

To know the ability of SH-SY5Y cells to maintain B[a]P-induced cellular function due to oxidative stress, the NPY expression was assessed. The study showed a significant increase in NPY expression following B[a]P treatment in SH-SY5Y human neuroblastoma cell line. The present findings suggested that NPY expression by the B[a]P-induced metabolites can be associated with regulation of cytoskeletal proteins. Previous studies showed the central NPY exerts protective effects under stress and is known to play an essential role in the basic mechanisms of stress tolerance by reducing anxiety and depressive-like behaviours [45,46]. B[a]P significantly increases NPY levels in the hypothalamus, and the hippocampus, which may leads to alteration in behavior [47,48]. Hence, B[a]P-induced neurotoxicity might provides new insight into the induction of serious neurodegenerative diseases following exposure to chemical pollutants that produced due to incomplete combustion of fossil fuel causing increasing load of anthropogenic neurotoxicants [49]. The present study also provide for the first time an experimental evidence that B[a]P exposure may stimulates the neuroblastoma SH-SY5Y cell lines to release functionally active NPY causing cell cycle arrest in S-phase by microtubule disruption and spindle formation that might be achieved through oxidative stress and ROS induced spindle abnormalities during cellular metabolism through intracellular calcium [50,51]. These findings identified a novel mechanism by which ROS regulate NPY expression and indicated a potential molecular target for the treatment of oxidative stress-related neurodegenerative diseases.

 doi:10.20944/preprints202003.0357.v1

## 5. Conclusion

In conclusion the endogenous NPY release into the hippocampus may induce a compensatory mechanism for neuronal survival after the oxidative damage induced by exposure to B[a]P in SH-SY5Y cell. The possible mechanism of this protection is that NPY may prevents human neuroblastoma SH-SY5Y cells from achieving mitosis and microtubule assembly inhibiting SH-SY5Y cell proliferation by a novel mechanism. However, NPY may not just be a mere marker of microtubule disruption during development and in metabolic stress. The present findings suggest that NPY may serve a physiological role in cell cycle arrest and play a potential proximal role to protect the cell from B[a]P-induced oxidative stress during cell division. More research is needed to elucidate the unknown mechanism of action of NPY in neuronal cell cycle regulation and spindle assembly. A thorough understanding of the role of the microtubule cytoskeleton in stress responses like B[a]P exposure has the potential to lead to larger therapeutic windows that target neurodegenerative disorders.

## Abbreviations

PAHs: Polycyclic aromatic hydrocarbons; B[a]P:Benzo[a]pyrene,DMSO: Dimethyl sulphoxide; FBS: Fetal Bovine Serum; DMEM: Dulbecco's modified Eagle medium; MTT: 3-(4,5-dimethylthiazol-2-yl)2,5-diphenyl-tetrazolium bromide; RA: Retinoic acid; CYP: Cytochrome P450; 8-oxodG: 8-oxo-deoxyguanosine; DAPI: 4′,6-diamidino-2-phenylindole; NPY: Neuropeptide Y; ROS: Reactive oxygen species

## Acknowledgements

The author acknowledged the financial support from BRNS, Mumbai & DRDO, Delhi.

## Authors' contributions

MP designed the protocol and performed the experiments with the image analysis. MP also interpreted the data and drafted the manuscript.

## Funding

This work was supported by grants from Board of Research in Nuclear Sciences (BRNS), Department of Atomic Energy (DAE), Government of India (No.37(1)/14/27/2015/BRNS) and DRDO, New Delhi, No. O/o DG (TM)/ 81/48222/LSRB-294/PEE&BS/2017

## Conflict of Interest

The author declared that there was no conflict of interest.

## Data availability

All data generated or analyzed during this study are included in the article.

 doi:10.20944/preprints202003.0357.v1

**References**


1. Guo Y., Wu K., Huo X, Xu X. Sources, distribution, and toxicity of polycyclic aromatic hydrocarbons. J Environ Health. 2011; 73(9):22-5.
2. Thamaraiselvan R., Peramaiyan R., Natarajan N., Boopathy L., Palaniswami R., Ikuo N. Exposure to polycyclic aromatic hydrocarbons with special focus on cancer. Asian Pac J Trop Biomed. 2015; 5(3):182-189.
3. Saunders CR., Ramesh A., Shockley DC. Modulation of neurotoxic behavior in F-344 rats by temporal disposition of B(a)P. Toxicol Lett. 2002;129(1-2):33-45.
4. Cheng SQ, Xia YY, He JL, Liu XQ, Chen XM, Ding YB, Wang YX, Peng B, Tu BJ. Neurotoxic effect of subacute benzo(a)pyrene exposure on gene and protein expression in rats. Environ Toxicol Pharmacol. 2013; 36(2):648-58.
5. Nie JS., Zhang HM., Zhao J., Liu HJ., Niu Q. Involvement of mitochondrial pathway in B[a]P-induced neuron apoptosis. Hum Exp Toxicol. 2014; 33(3):240-50.
6. Das SK., Patri M. Neuropeptide Y expression confers benzo[a]pyrene induced anxiolytic like behavioral response during early adolescence period of male Wistar rats. Neuropeptides. 2017; 61: 23-30.
7. Mohanty R., Das SK., Patri M. Modulation of benzo[a]pyrene induced anxiolytic-like behavior by retinoic acid in zebrafish: involvement of oxidative stress and antioxidant defense system. Neurotox Res. 2017;31:493-504
8. Patel B., Das SK., Patri M. Neonatal benzo[a]pyrene exposure induces oxidative stress and DNA damage causing neurobehavioural changes during the early adolescence period in rats. Dev Neurosci. 2016b;38(2):150-62.
9. Yan C., Zhang D., Raygoza Garay J A., Mwangi MM & Bai L. Decoupling of divergent gene regulation by sequence-specific DNA binding factors. Nucleic Acids Res. 2015; 43, 7292-7305.
10. Yuan L., Lv B., Zha J., Wang Z. Benzo[a]pyrene induced p53-mediated cell cycle arrest, DNA repair, and apoptosis pathways in Chinese rare minnow (*Gobiocypris rarus*). Environ Toxicol. doi: 2016; 10.1002/tox.22298.
11. Patel S., Bajpayee M., Pandey A., Parmar D., Dhawan A. In vitro induction of cytotoxicity and DNA strand breaks in CHO cells exposed to cypermethrin, pendimethalin, and dichlorovous. Toxicol In vitro. 2007;

21:1409–12.

12. Mohanty R., Das SK., Singh NR., Patri M. Withania somnifera leaf extract ameliorates B[a]P-induced behavioral and neuromorphological alterations by improving brain antioxidant status in zebrafish (*D. rerio*), Zebrafish. 2016; 13(3):188-96.
13. Das SK., Patel B., Patri M. Neurotoxic Effect of Benzo[a]pyrene and its possible association with 6-Hydroxydopamine induced neurobehavioral changes during early adolescence period in rats. J Toxicol. 2016:8606410.
14. Nicoletti I., Migliorati G., Pagliacci MC., Grignani F, Riccardi C. A rapid and simple method for measuring thymocyte apoptosis by propidium iodide staining and flow cytometry. J Immunol Methods. 1991; 139:271-9.
15. Hemant Kumar, Hyung-Woo Lim, Sandeep Vasant More, Byung-Wook Kim, Sushruta Koppula, In Su Kim, Dong-Kug Choi The Role of Free Radicals in the Aging Brain and Parkinson's Disease: Convergence and Parallelism, Int J Mol Sci. 2012; 13(8): 10478–10504.
16. Parker AL, Kavallaris M, McCarroll JA. Microtubules and their role in cellular stress in cancer. Front Oncol. 2014 Jun 18;4:153. doi: 10.3389/fonc.2014.00153
17. Köhler, S.; Schaller, V.; Bausch, A.R. Collective dynamics of active cytoskeletal networks. PLoS ONE 2011, 6.
18. Roediger B, Armati PJ. Oxidative stress induces axonal beading in cultured human brain tissue. Neurobiol Dis 2003; 13(3):222–910.
19. Winters L, Ban I, Prelogović M, Kalinina I, Pavin N, Tolić IM.Pivoting of microtubules driven by minus-end-directed motors leads to spindle assembly. BMC Biol. 2019 May 23;17(1):42. doi: 10.1186/s12915-019-0656-2
20. Hinshaw SM, Harrison SC. Kinetochore Function from the Bottom Up. Trends Cell Biol. 2018; 28(1):22–33. DOI: 10.1016/j.tcb.2017.09.002.
21. Shipley MM., Mangold CA., Szpara ML. Differentiation of the SH-SY5Y Human Neuroblastoma Cell Line. J Vis Exp. 2016; (108):53193.
22. McDonald R. L., Vaughan P.F.T., Beck-Sickinger A.G., Peers C. Inhibition of $Ca^{2+}$ channel currents in human neuroblastoma (SH-SY5Y) cells by NPY and a novel cyclic NPY analogue, Neuropharmacology;1995;34: 11, November, Pages 1507-1514.
23. Wu YF and Li SB. Neuropeptide Y expression in mouse hippocampus and

its role in neuronal excitotoxicity. Acta Pharmacol Sin. 2005; 26, 63-68.

24. Attoff, K., Kertika, D., Lundqvist, J., Oredsson, S., Forsby, A. Acrylamide affects proliferation and differentiation of the neural progenitor cell line C17.2 and the neuroblastoma cell line SH-SY5Y. Toxicol. In. Vitro. 2016a; 35, 100-111.
25. Causing CG, Makus KD, Ma Y, Miller FD, Colmers WF Selective up regulation of T alpha 1 alpha-tubulin and neuropeptide Y mRNAs after intermittent excitatory stimulation in adult rat hippocampus in vivo. J Comp Neurol. 1996;Mar 25;367(1):132-46.
26. Gotzsche, CR., and Woldbye, DP. The role of NPY in learning and memory. Neuropeptides. 2016; 55, 79–89. doi: 10.1016/j.npep.2015.09.010
27. Reichmann F and Holzer P. Neuropeptide Y: a stressful review. Neuropeptides. 2016; 55 pp 99-109.
28. Ross RA., Spengler BA., Biedler JL. (Coordinate morphological and biochemical inter conversion of human neuroblastoma cells. J Natl Cancer Inst. 1983; 71:741–9.
29. Fjaeraa C., Nånberg E. Effect of ellagic acid on proliferation, cell adhesion and apoptosis in SH-SY5Y human neuroblastoma cells. Biomed Pharmacother. 2009; 63(4):254-261.
30. Chiappini C., Berliocchi L., Cerri S., et al. Early LC3 lipidation induced by d-limonene does not rely on mTOR inhibition, ERK activation and ROS production and it is associated with reduced clonogenic capacity of SH-SY5Y neuroblastoma cells. Phytomedicine. 2018; 40:98-105.doi:10.1016/j.phymed.. 01.005.
31. Ganem NJ, Pellman D. Linking abnormal mitosis to the acquisition of DNA damage. J Cell Biol. 2012; 199(6):871-81
32. Dvorák Z., Vrzal R., Ulrichová J., Pascussi JM., Maurel P., Modriansky M. Involvement of cytoskeleton in AhR-dependent CYP1A1 expression. Curr Drug Metab. 2006; 7(3):301-13.
33. Stellas D., Souliotis VL., Bekyrou M., Smirlis D., Kirsch-Volders M., Degrassi F., Cundari E., Kyrtopoulos SA. B[a]P-induced cell cycle arrest in HepG2 cells is associated with delayed induction of mitotic instability. Mutat Res. 2014;769:59-68.
34. Goldman RL., Canterberry M., Borckardt JJ., Madan A., Byrne TK., George

 doi:10.20944/preprints202003.0357.v1

MS., O'Neil PM., Hanlon CA. Executive control circuitry differentiates degree of success in weight loss following gastric-bypass surgery. Obesity Silver Spring. 2013; 21(11):2189–2196

35. Patri M and Singh A. Protective effects of noradrenaline on benzo[a]pyrene-induced oxidative stress responses in brain tumor cell lines, *In Vitro* Cellular & Developmental Biology-Animal. 2019; 55:665–675.
36. Patri M., Singh A., Mallick BN. Protective role of noradrenaline in B[a]P-induced learning impairment in developing rat. J Neurosci Res.2013; 91(11):1450-62.
37. Kormos V., and Gaszner B. Role of neuropeptides in anxiety, stress, and depression: From animals to humans. Neuropeptides. 2013;Vol. 47, Issue 6, 401-419.
38. Le Ferrec E., Lagadic-Gossmann D., Rauch C., Bardiau C., Maheo K., Massiere F., Le Vee M., Guillouzo A., Morel F. Transcriptional induction of CYP1A1 by oltipraz in human Caco-2 cells is aryl hydrocarbon receptor- and calcium-dependent. J Biol Chem. 2002; 277(27):24780-7.
39. Bouayed J., Bohn T., Tybl E., Kiemer AK., Soulimani R Benzo[α]pyrene-induced anti-depressive-like behaviour in adult female mice: role of monoaminergic systems. Basic Clin Pharmacol Toxicol. 2012;110(6):544-50.
40. Patel B., Das SK., Das S., Das L., Patri M. Neonatal exposure to benzo[a]pyrene induces oxidative stress causing altered hippocampal cytomorphometry and behavior during early adolescence period of male Wistar rats. Int J Dev Neurosci. 2016a 50:7-15.
41. Fang, C., Kuo, H., Hsu, S. et al. HSP70 is required for the proper assembly of pericentriolar material and function of mitotic centrosomes. Cell Div 2019;14, 4
42. Zhang W., Tian F., Zheng J., Li S., Qiang M. Chronic administration of B(a)P induces memory impairment and anxiety-like behavior and increases of NR2B DNA methylation. PLoS One. 2016; 11(2): e0149574.
43. IPCS. Environmental Health Criteria for Boron, (1998) vol.204, World Health Organization, Geneva.
44. Hood DB., Ramesh A., and Aschner M. Polycyclic aromatic hydrocarbons: Exposure from emission products and terrorist attacks on US targets: Implications for developmental CNS toxicity. In: Handbook of Toxicology of

 doi:10.20944/preprints202003.0357.v1

Chemical Warfare Agents, ed. R.C. Gupta. London, U.K.: Academic Press, 2009; pp. 229-243.

45. Andrysík Z., Vondrácek J., Machala M., Krcmár P., Svihálková-Sindlerová L., Kranz A., Weiss C., Faust D., Kozubík A., Dietrich C. The aryl hydrocarbon receptor-dependent deregulation of cell cycle control induced by polycyclic aromatic hydrocarbons in rat liver epithelial cells. Mutat Res. 2007; 615(1-2):87-97.
46. Binková B., Giguère Y., Rössner P Jr., Dostál M., Srám RJ. The effect of dibenzo[a,1]pyrene and benzo[a]pyrene on human diploid lung fibroblasts: the induction of DNA adducts, expression of p53 and p21(WAF1) proteins and cell cycle distribution. Mutat Res. 2000; 471(1-2):57-70.
47. Jeffy BD., Chen EJ., Gudas JM., Romagnolo DF. Disruption of cell cycle kinetics by benzo[a]pyrene: inverse expression patterns of BRCA-1 and p53 in MCF-7 cells arrested in S and G2. Neoplasia. 2000;2(5):460-70.
48. Silva AP., Kaufmann JE., Vivancos C., Fakan S., Cavadas C., Shaw P., Brunner HR., Vischer U., Grouzmann E. Neuropeptide Y expression, localization and cellular transducing effects in HUVEC. Biol Cell. 2005; 97(6):457-6
49. Pons J., Kitlinska J., Jacques D., Perreault C., Nader M., Everhart L., Zhang Y., Zukowska Z. Interactions of multiple signalling pathways in NPY-mediated bimodal vascular smooth muscle cell growth. Can J Physiol Pharmacol. 2008; 86(7):438 48.
50. Baldock PA., Lin S., Zhang L et al. Neuropeptide Y attenuates stress-induced bone loss through suppression of NE circuits. J Bone Miner Res. 2014; 29:2238-2249.
51. Mihara S., Shigeri Y., Fujimoto M. Neuropeptide Y-induced intracellular $Ca^{2+}$ increases in vascular smooth muscle cells FEBS Lett. Dec.1989; 18; 259(1):79-82.
52. Simonneaux V., Rodeau JL., Calgari C., Pévet P. Neuropeptide Y increases intracellular calcium in rat pinealocytes. Eur J Neurosci. 1999; Feb 11(2):725-8.

Preprints (www.preprints.org) | NOT PEER-REVIEWED | Posted: 24 March 2020 doi:10.20944/preprints202003.0357.v1

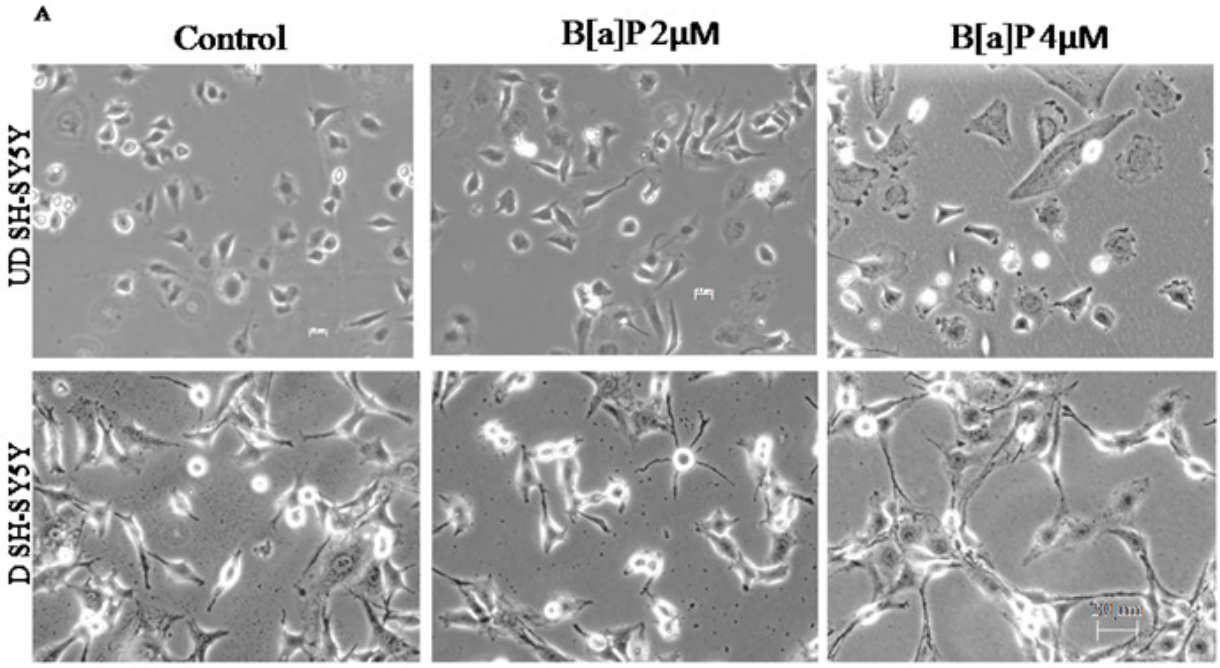


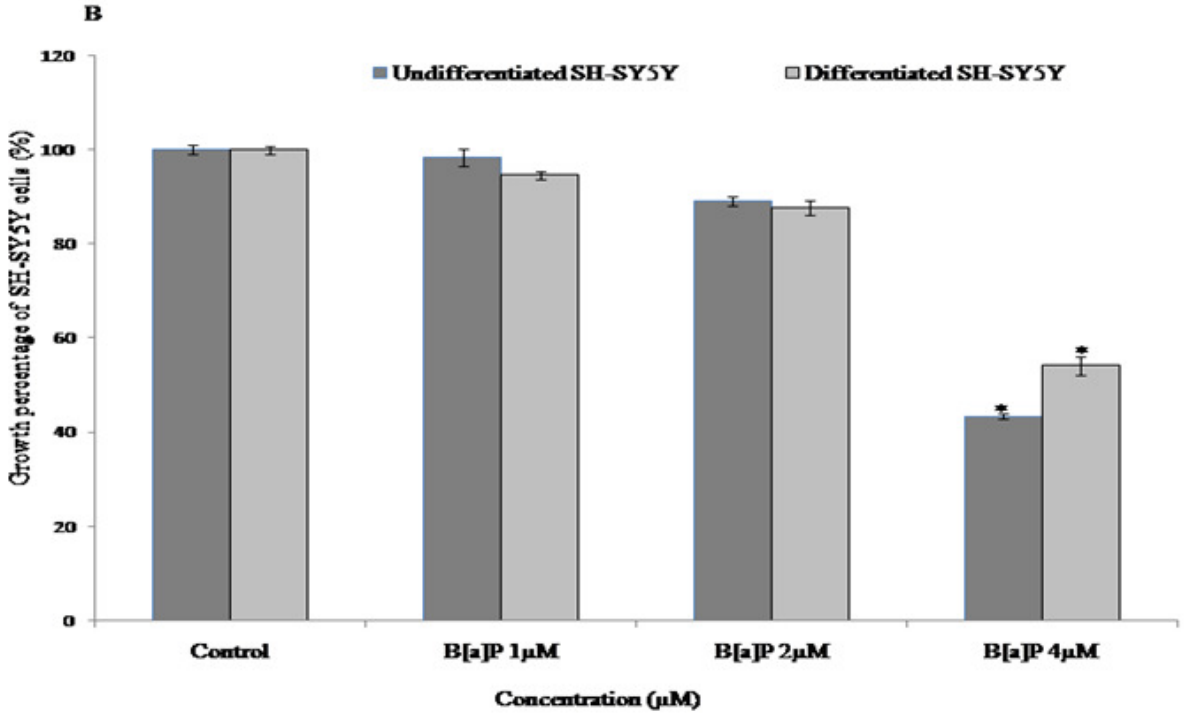


**Figure 1**

Preprints (www.preprints.org) | NOT PEER-REVIEWED | Posted: 24 March 2020 doi:10.20944/preprints202003.0357.v1

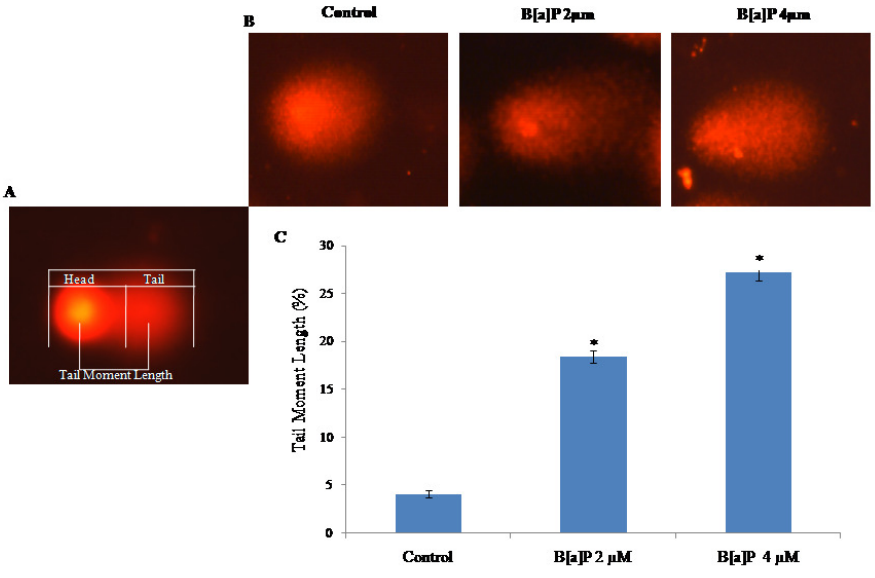


Figure 2

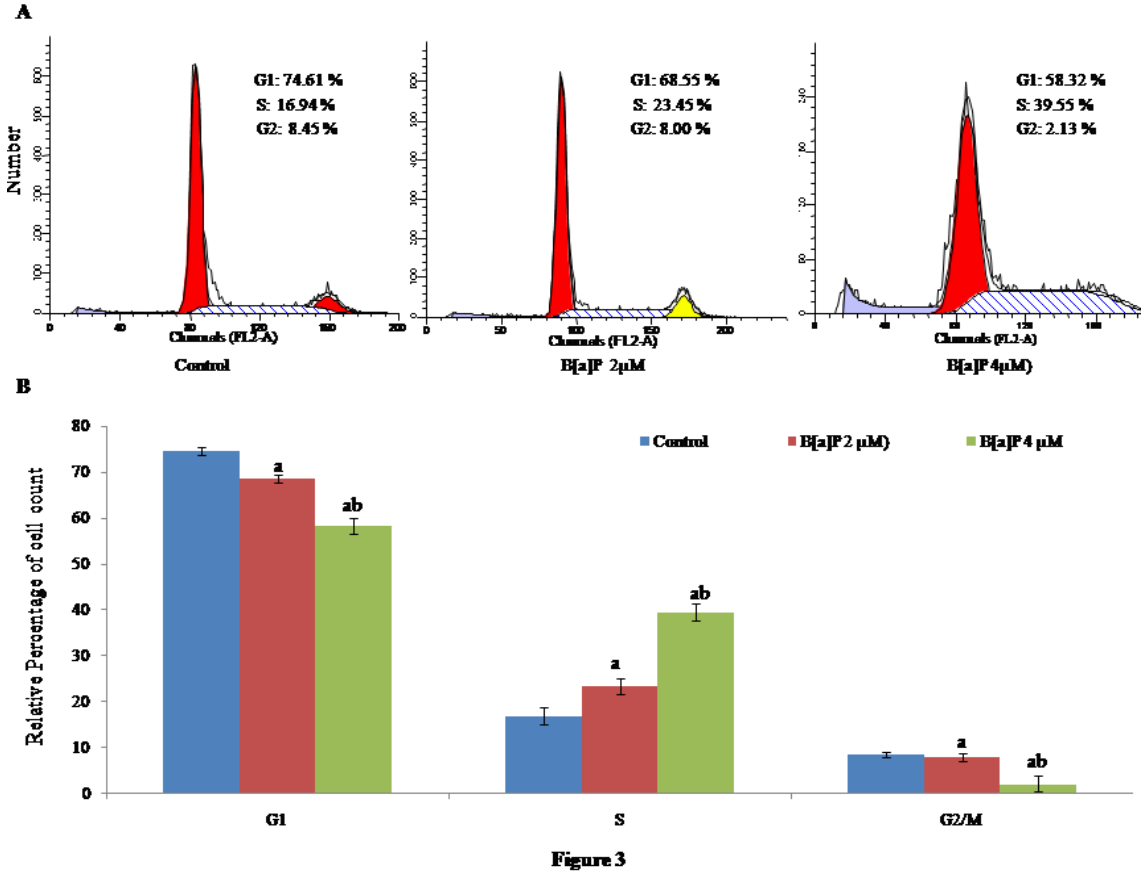


Figure 3

Preprints (www.preprints.org) | NOT PEER-REVIEWED | Posted: 24 March 2020 doi:10.20944/preprints202003.0357.v1

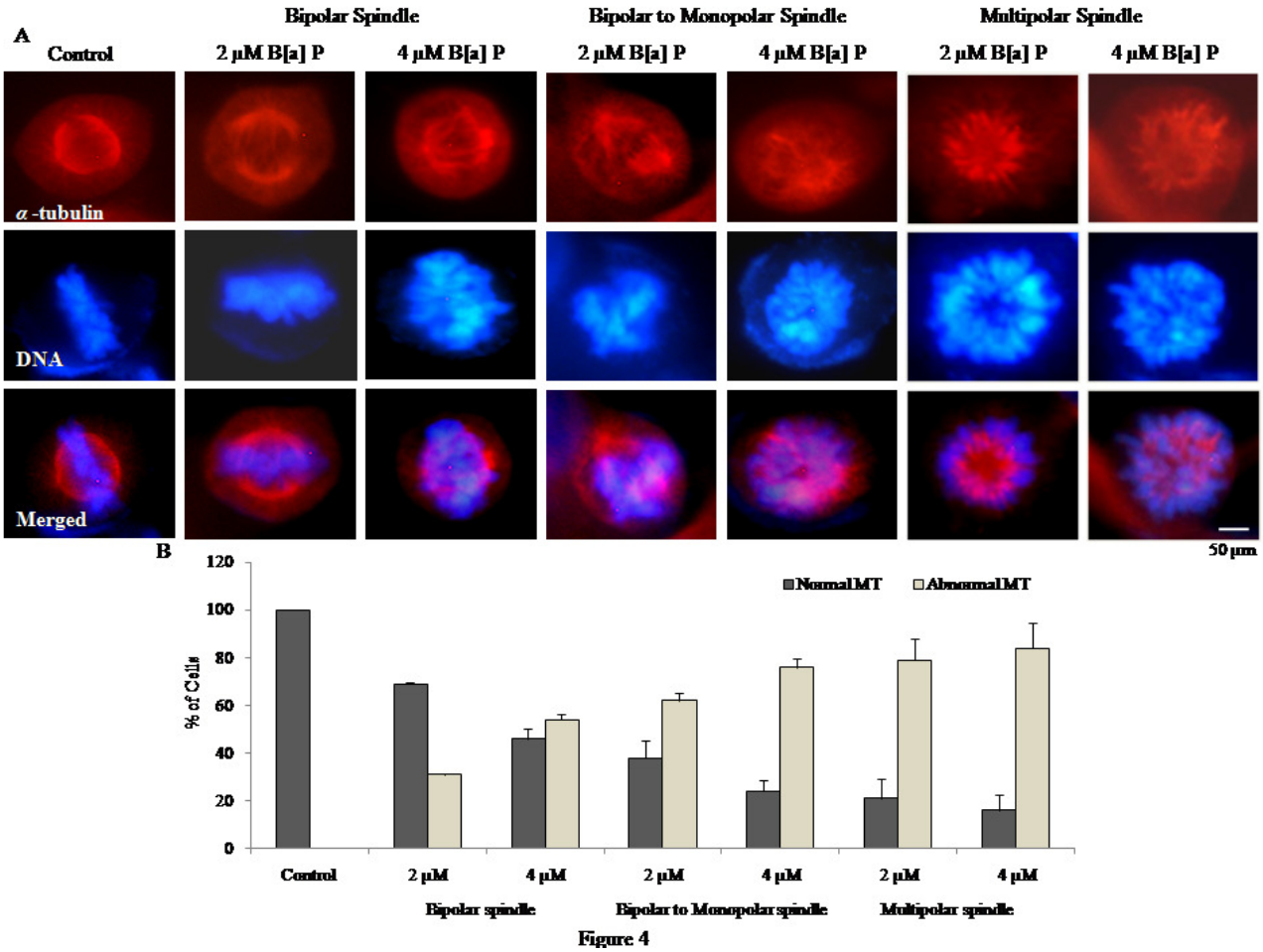


Figure 4

Preprints (www.preprints.org) | NOT PEER-REVIEWED | Posted: 24 March 2020 doi:10.20944/preprints202003.0357.v1

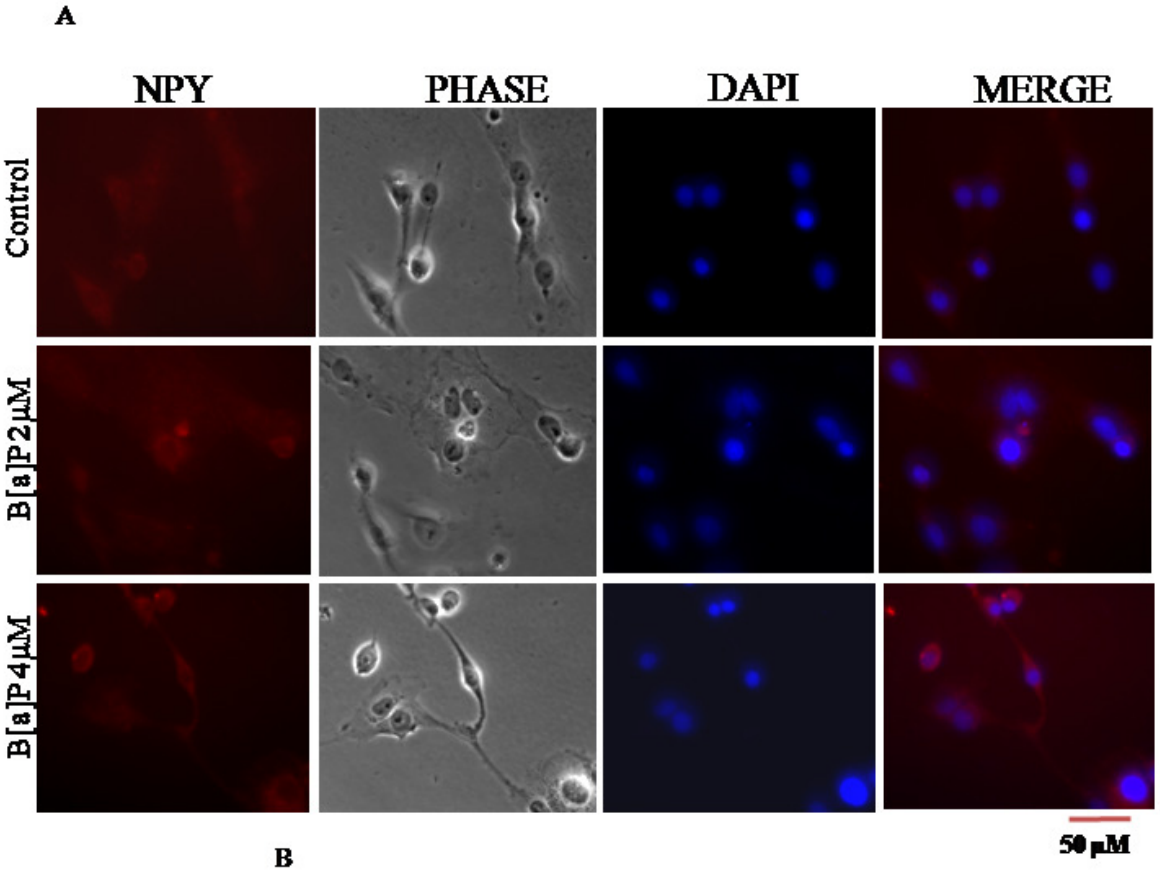


Figure 5

Preprints (www.preprints.org) | NOT PEER-REVIEWED | Posted: 24 March 2020 doi:10.20944/preprints202003.0357.v1

**Figure Legends:**

**Figure 1. Cell viability assay**:

Phase contrast microscopy images showing the morphological changes in SH-SY5Y cells after treatment with B[a]P in 1% serum-supplemented medium. Morphological appearance of undifferentiated (UD) and differentiated (D) SH-SY5Y cells, where undifferentiated SH-SY5Y cells have a flat phenotype with few projections (Fig. 1A). Differentiated SH-SY5Y neurons demonstrate extensive and elongated neuritic projections. Images were obtained in phase at 20x magnification using an inverted epifluorescence microscope from three independent cell preparations. Affect of RA treatment on cultured SH-SY5Y cells (Fig. 1A) Light microscopy micrographs of undifferentiated cells and 10μM RA differentiated cells (lower panel). A change in cell phenotype with extensive neurite outgrowth was observed.

SH-SY5Y cells treated with various concentrations of B[a]P (1, 2, and 4μM) for 24 hours. Percentage of cell viability to different doses of B[a]P (Fig. 1B) exposure. The UD and D SH-SY5Y cells display different vulnerability to cytotoxicity of B[a]P. The dose effect curves of B[a]P-exposed SHSY5Y cells on growth diverged as the dose (2 and 4μM) increased and the cell viability decreased, which indicated that B[a]P exerted a significant toxic effect on both undifferentiated and differentiated SHSY5Y cells; (n=3) (Fig 1B). Data were shown as mean ± SEM, * indicates significant difference (*$p < 0.05$) respect to comparison between groups.

**Figure 2. Effect of B[a]P-induced DNA damage in SH-SY5Y cells**

Representative photomicrograph of PI fluorescence of SH-SY5Y cells showing DNA damage with comet head and tail (Fig 2A). DNA damage was shown after 24hrs of different doses of B[a]P treatment with comet tail having fragmented DNA and extensive DNA migration indicating B[a]P induced DNA strand breaks where as control cells showed intact very bright nuclei with slight or no DNA migration in SH-SY5Y (Fig 2B) and extent of DNA migration was quantified in tail moment length. Histogram for tail moment length in SH-SY5Y cells under control and different doses of B[a]P treated conditions were also shown (Fig 2C). The tail moment was calculated as a product of tail length and fraction of the DNA in the tail using the image analysis system of Comet Score™ v1.5 (TriTek Corp., USA). Fifty randomly chosen comets were analysed in each group and data are expressed as the mean ± SEM from three independent experiments (n=3). Significant difference (*$p<0.05$); Scale bar: 40 μm.

Preprints (www.preprints.org) | NOT PEER-REVIEWED | Posted: 24 March 2020 doi:10.20944/preprints202003.0357.v1

**Figure 3. Cell cycle analysis after B[a]P exposure**

Flow cytometry was performed to analyze apoptosis. Representative flow cytometry profiles of DNA content in human SH-SY5Y neuroblastoma cells stained with propidium iodide, showing cell-cycle following treatment with different doses of B[a]P; Control (DMSO); 2μM and 4μM B[a]P, each for 24 hour at 37ºC (Fig 3A).

Percentage of apoptotic cells in SH-SY5Y neuroblastoma cells in G2/M phase following treatment with B[a]P (2 and 4 μM) for 24 h at 37ºC. B[a]P treatment to SH-SY5Y neuroblastoma cells showed significant increase in percentage of cells in S and G2/M phases of cell cycle as compared to G1 (Fig. 3B). Statistical significance was measured using one way ANOVA followed by post hoc analysis with Newman-Keul's test (Sigma Stat software, Jandel Scientific USA). Values are expressed as mean ± SEM. 'a' and 'b' denotes $p<0.05$ when compared to control group. Data presented as Mean ± SD of three independent experiments.

**Figure 4. B[a]P-induced tubulin arrangement in mitotic spindle**

Immunofluorescence of SH-SY5Y cells showing B[a]P induced mitotic spindle destabilisation (Fig 4). Immunofluorescence images of control (DMSO) and different doses of B[a]P treated (2 or 4μM) SH-SY5Y cells for 24 hours with disoriented spindle arrangement were shown with tubulin (red) and DNA (DAPI-blue) staining (Fig. 4A). Quantitative of fluorescence intensity at the spindle region showing percentage of cells in normal and abnormal mitotic spindle arrangement in control and different doses of B[a]P treated cells (Fig. 4B). Values are the mean ± SE of 3 independent experiments. Scale bar: 10μM, magnification: 60X

**Figure 5. Effect of B[a]P on NPY protein expression in SH-SY5Y cells by immunofluorescence**.

Immunostaining of a representative from SH-SY5Y cells showing immunostaining for anti-NPY antibody reported to specifically detect NPY in neuroblastoma cells. The immunoreactivity were observed in B[a]P treated SH-SY5Y cells after exposure to B[a]P for 24 hours. Representative images showing the distribution of NPY (red) and chromosome (blue) in SH-SY5Y cells; overlay with DAPI (to counterstain the nuclei; blue) and merged with control and B[a]P treated groups (Fig. 5A). Quantification of fluorescence intensities for NPY-specific immunoreactions in two different doses of B[a]P treatment (Fig. 5B). Data were shown as mean ± SEM; * indicates significant difference ($*p < 0.05$) respect to comparison between groups. Scale bars=50μm.

Preprints (www.preprints.org) | NOT PEER-REVIEWED | Posted: 24 March 2020 doi:10.20944/preprints202003.0357.v1

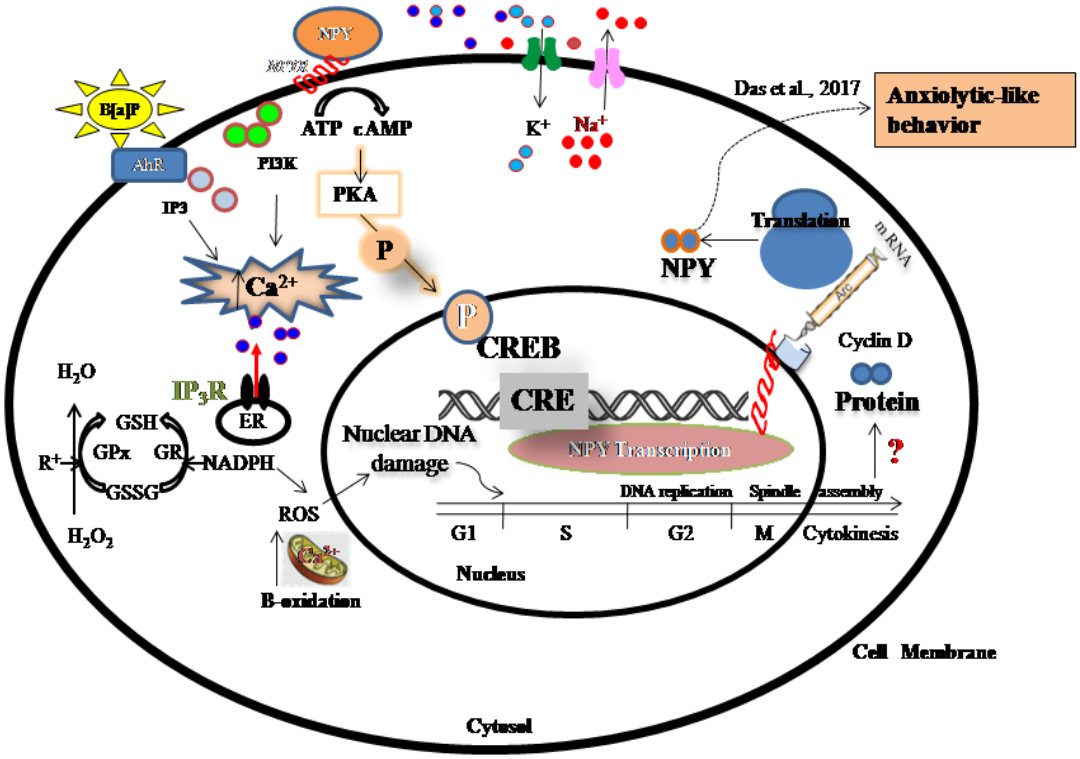


**Figure: Graphical abstract**

**Graphical abstract:**

Schematic diagram of the signalling pathways that mediate behavioral phenotypes induced by B[a]P exposure showing elevated expression of Neuropeptide Y (NPY). NPY is the most abundant peptide found in the mammalian brain and it plays an important role in the regulation of the HPA axis and energy homeostasis in human biological processes. NPY needs to bind to the NPY receptor to activate the specific signalling pathways. Elevated NPY binding with its receptors up regulates the influx of calcium through activation of the small G protein. B[a]P-induced intracellular calcium increase and the occurrence of reactive oxygen species being transported into the mitochondria for β-oxidation, particularly stimulating NPY synthesis in hippocampus. Increased release of NPY in inhibits sympathetic nerve system (SNS) outflow resulting in mitochondrial oxidative stress that causes DNA damage during different cell cycle phases showing spindle abnormalities with disorganized arrays of microtubules spindle disorientation. The activities of nuclear transcription factors are stimulated by dephosphorylated and phosphorylated CREB (cAMP response element binding) protein, which then induce the cell cycle arrest and thereafter may trigger anxiolytic-like behavioral responses.